HHS Public Access

Author manuscript

Eur J Nucl Med Mol Imaging. Author manuscript; available in PMC 2023 January 08.

Published in final edited form as:

Eur J Nucl Med Mol Imaging. 2022 September ; 49(11): 3679–3691. doi:10.1007/s00259-022-05825-6.

Imaging the fetal nonhuman primate brain with SV2A positron emission tomography (PET)

Samantha Rossano[1,2], **Takuya Toyonaga**[1], **Eric Berg**[3], **Isabella Lorence**[1], **Krista Fowles**[1], **Nabeel Nabulsi**[1], **Jim Ropchan**[1], **Songye Li**[1], **Yunpeng Ye**[1], **Zachary Felchner**[1], **David Kukis**[4], **Yiyun Huang**[1], **Helene Benveniste**[5], **Alice F. Tarantal**[6], **Stephanie Groman**[7,8], **Richard E. Carson**[1,2]

[1]Department of Radiology and Biomedical Imaging, Yale PET Center, Yale School of Medicine, New Haven, CT, USA

[2]Department of Biomedical Engineering, Yale University, New Haven, CT, USA

[3]Department of Biomedical Engineering, University of California, Davis, CA, USA

[4]Center for Molecular and Genomic Imaging, University of California, Davis, CA, USA

[5]Department of Anesthesiology, Yale School of Medicine, Yale University, New Haven, CT, USA

[6]Departments of Pediatrics and Cell Biology and Human Anatomy, School of Medicine, and California National Primate Research Center, University of California, Davis, CA, USA

[7]Department of Psychiatry, Yale University, New Haven, CT, USA

[8]Department of Neuroscience, University of Minnesota, Minneapolis, MN, USA

Abstract

Purpose—Exploring synaptic density changes during brain growth is crucial to understanding brain development. Previous studies in nonhuman primates report a rapid increase in synapse number between the late gestational period and the early neonatal period, such that synaptic density approaches adult levels by birth. Prenatal synaptic development may have an enduring impact on postnatal brain development, but precisely how synaptic density changes in utero

✉Samantha Rossano, samantha.rossano@yale.edu.

Author contribution SR collected and analyzed PET data, completed Western blotting and analysis, and prepared manuscript; TT supervised Western blotting and analysis, and manuscript preparation; EB collected and reconstructed PET data; IL analyzed PET data; KF performed PET imaging and data collection; NN, JR, SL, YY, ZF, and HH developed, synthesized, and QC of PET tracers; DK synthesized PET tracers; HB contributed to study design; AFT identified and assigned animals, performed all monitoring and imaging including ultrasound and PET/CT, data collection, performed all fetal tissue collections, contributed to study design, and manuscript preparation; SG analyzed PET data, contributed to study design, and manuscript preparation; REC contributed to study design, performed PET experiments, data analysis, and manuscript preparation.

Supplementary Information The online version contains supplementary material available at https://doi.org/10.1007/s00259-022-05825-6.

Code of Availability The code used in the current study will be made available upon reasonable request to the corresponding and participating authors as deemed appropriate, and in line with the data sharing policy.

Ethics approval All procedures were carried out in strict accordance to the guidelines set forth in the Animal Welfare Act and the Guide for the Care and Use of Laboratory animals. All animal procedures were approved prior to implementation by Yale University's Institutional Animal Care and Use Committee (IACUC) and by the IACUC at the University of California, Davis.

Conflict of interest The authors declare no competing interests.

are unknown because current methods to quantify synaptic density are invasive and require post-mortem brain tissue.

Methods—We used synaptic vesicle glycoprotein 2A (SV2A) positron emission tomography (PET) radioligands [^{11}C]UCB-J and [^{18}F]Syn-VesT-1 to conduct the first assessment of synaptic density in the developing fetal brain in gravid rhesus monkeys. Eight pregnant monkeys were scanned twice during the third trimester at two imaging sites. Fetal post-mortem samples were collected near term in a subset of subjects to quantify SV2A density by Western blot.

Results—Image-derived fetal brain SV2A measures increased during the third trimester. SV2A concentrations were greater in subcortical regions than in cortical regions at both gestational ages. Near term, SV2A density was higher in primary motor and visual areas than respective associative regions. Post-mortem quantification of SV2A density was significantly correlated with regional SV2A PET measures.

Conclusion—While further study is needed to determine the exact relationship of SV2A and synaptic density, the imaging paradigm developed in the current study allows for the effective in vivo study of SV2A development in the fetal brain.

Keywords

Synaptogenesis; In utero; Positron emission tomography; SV2A; Nonhuman primate

Introduction

Synapses, or connections between neurons, are essential to proper brain function, which relies on neurotransmission of nerve impulses to propagate signals. The process of synaptogenesis, or the formation of synapses, begins during mid-gestation in nonhuman primates (NHP) and humans [1–3], and persists through the early postnatal period across the macaque cortex [4–8]. Previous studies have quantified synaptic density during critical periods of brain development in the post-mortem NHP brain using ex vivo approaches, such as electron microscopy. These studies have observed a profound increase in synaptic density during the second half of gestation that approaches levels observed in adults by the time of birth and exceed adult levels in the first four postnatal months. Gestational synaptogenesis is believed to be critical for subsequent brain development and has been proposed to be a mechanism by which mental health challenges emerge [9–12]. Direct evidence to support this hypothesis, however, has been limited because these ex vivo measures of synaptic density cannot be repeatedly assessed in the same subject, and thus cannot follow a single subject longitudinally across the developmental trajectory.

An alternative approach is in vivo imaging of synapses. Positron emission tomography (PET) is an imaging modality in which radioactive ligands are used to image and quantify particular proteins of interest in living tissue. Kinetic analysis of these images can provide valuable physiological information regarding the distribution of the target protein of interest. Recently, innovations in the field of PET have focused on imaging the synaptic vesicle glycoprotein 2A, SV2A, which is expressed on presynaptic vesicles across the central nervous system [13]. In particular, two PET radioligands, [^{11}C]UCB-J [14] and [^{18}F]SynVesT-1 [15], have been developed to image SV2A in both NHP and humans

and have been used to investigate synaptic density differences in human participants with Alzheimer's disease [16, 17], depression [18], and epilepsy [19]. Although the relationship between SV2A expression and synapse number per unit area is not fully understood, SV2A co-localizes with synaptophysin (SYN), a commonly used synaptic density marker. Furthermore, SV2A PET measures in the baboon have been shown to correlate well with ex vivo synaptic density markers of SV2A and SYN [20]. Thus, SV2A PET is a powerful tool to noninvasively measure synaptic density in vivo.

In the current study, we sought to demonstrate the potential of SV2A PET imaging to longitudinally assess prenatal brain development. Pregnant rhesus monkeys underwent two SV2A PET scans at mid and late gestation to assess SV2A density in the fetal brain. Brain tissue was collected from a subset of fetuses for post-mortem analyses with Western Blot. Our goal was to compare SV2A PET measures to the patterns and synaptic density levels relative to adult measures that have been reported in previous ex vivo literature. We hypothesized that SV2A PET measures would increase in the fetal brain during this period, approaching the adult SV2A PET uptake levels in vivo. For this study, PET imaging data were collected across two imaging sites. The first site (Yale PET Center, Yale University, New Haven, CT) studied four gravid rhesus macaques with two scans during the third trimester of gestation with [^{11}C]UCB-J at 119 (± 6) and 147 (± 4) gestational days. The second site (Multimodal Imaging Core at the California National Primate Research Center, University of California, Davis, Davis, CA) studied four gravid rhesus macaques scanned twice during the third trimester with [^{18}F]SynVesT-1 at 125 (± 4) and 143 (± 3) gestational days. Together, images from both cohorts were quantified to explore and validate regional SV2A changes in the developing fetal rhesus brain. These data indicate the feasibility of longitudinal imaging with SV2A PET in the prenatal monkey and provide insight into the key process of synaptogenesis in the developing brain.

Materials and methods

Rhesus monkeys and SV2A PET image acquisition

A total of eight gravid rhesus monkeys were included in these studies. Rhesus monkeys were scanned at two gestational ages during the third trimester (111–165 days; term 165 ± 10 days), once at approximately 120 days and once at approximately 145 days. At the first scanning site, four female NHP underwent PET scanning with [^{11}C]UCB-J (185 MBq) at the Yale PET Center (Site 1, Yale University School of Medicine, New Haven, CT). At the second scanning site, a cohort of four animals underwent PET scanning with [^{18}F]SynVesT-1 (111 MBq) at the California National Primate Research Center at the University of California at Davis (Site 2). Table 1 and Online Resource 1 describe the sedation, scanning, and image reconstruction methods used at each scan site. At Site 1, PET/CT images were acquired on the Siemens Biograph mCT. Dams were sedated with ketamine/glycopyrrolate (7–10 mg/kg) and maintained under gas anesthesia (isoflurane; 0.75–2.5%) for the duration of the scan. PET images were reconstructed using time of flight (TOF) + point spread function (PSF) modeling and ordered subset expectation maximization (OSEM) algorithm with 3 iterations of 21 subsets (Siemens Medical Solutions, USA). At Site 2, female rhesus monkeys were identified as pregnant according to established

ultrasound methods [21]. Prior to study assignment, normal embryonic/fetal growth and development were confirmed by ultrasound [21]. Fetuses were monitored sonographically across gestation including immediately prior to each PET/CT imaging session (120 and 145 days gestational age). Dams were sedated with telazol (5–8 mg/kg) supplemented with ketamine for each PET/CT session. The dams were carefully positioned for the CT scan (GE Discovery 610®) followed by PET imaging on the primate total-body PET imaging system (mini-EXPLORER) [22, 23]. PET images were reconstructed using list-mode TOF + PSF modeling and OSEM with 2 iterations of 21 subsets [23]. At both sites, all procedures were carried out in strict accordance to the guidelines set forth in the Animal Welfare Act and the Guide for the Care and Use of Laboratory Animals.

SV2A image processing and quantification

Since animals were sedated for the full duration of the PET scan, dynamic images had no evidence of motion artifacts in the fetal or maternal brain, and thus, the images were not corrected for motion. CT images were used to manually define fetal and maternal whole brain regions of interest (ROIs, Online Resource 2). Additionally, for the maternal brain, a threshold was applied to a summed PET image (30–60 min) to define voxels of maternal gray matter (GM). Time activity curves (TACs) of the maternal GM and the whole fetal brain were used for kinetic modeling analysis.

To determine regional SV2A PET uptake in the fetal brain, PET images were registered to regional templates (Neonate Rhesus Monkey template [24] and Adult Rhesus [25]) as described in Online Resource 1. These transformations were used to define the following regions of the fetal brain: prefrontal, frontal, parietal, occipital, temporal, subcortical (including thalamus, hypothalamus), hippocampus, amygdala, caudate, putamen, and cerebellum. Functional regions of interest include primary and associative auditory, motor, somatosensory, and visual cortices. TACs from these regions were used for the kinetic modeling analysis. Example TACs are shown in Online Resource 3A. TACs of regional and whole fetal brain uptake of the SV2A PET tracer were quantified using the reference Logan graphical analysis method [26], in which the dynamic PET data from a target region and a reference region are transformed to a linear equation to estimate the DVR between the target and reference tissues Using a t^* value of 10 min and the maternal GM as a reference region. Example Logan plots are shown in Online Resource 3B. The Logan method has also been used to noninvasively quantify dopamine transporter density in the striatum of the fetal brain using [^{18}F]Fallypride PET [27]. As the maternal GM has a very large concentration of SV2A, DVR is a measure of the relative specific (V_S) plus nonspecific (V_{ND}) tracer binding in the fetal and maternal brain. All but five scans utilized 60 min of dynamic PET data for kinetic analysis. In some ($N = 5$) scans at Site 2, kinetic analysis was shortened to 40 min as radioactivity estimates in the fetal brain were significantly affected by radioactivity collecting in the maternal bladder, due to fetal positioning in the maternal abdomen. DVR estimates using 40 min of data correlated well with estimates using 60 min (Online Resource 3C). Additional methods for kinetic analysis are described in Online Resource 1.

Changes in DVR within subject were explored across each of the aforementioned regions, as well as for cortical regions (average of prefrontal, frontal, parietal, occipital, temporal, and

cerebellum) and subcortical regions (average of thalamus, hippocampus, amygdala, caudate, putamen). Synaptogenesis rate (SR) was calculated as the change in DVR values from 120- to 145-days gestational age, normalized between scanning ages as shown below:

$$Synaptogenesis\,Rate\left(SR\right) = \frac{DVR_{scan2} - DVR_{scan1}}{Gestational\,age_{scan2} - Gestational\,age_{scan1}}$$

Regional synaptogenesis rate (rSR) values were calculated for 6 of the 8 total subjects using the DVR estimates from the Logan plot for each ROI from each scan. Two animals were excluded due to short interscan intervals, where scans 1 and 2 were ≤ 15 days apart. The remaining subjects' age difference between scans was 25 (± 5) days.

Parametric images of DVR were created by voxel-wise fitting of 10–60 min of dynamic PET data with reference Logan graphical analysis. These parametric images were resliced into template space and were used to calculate voxel-wise within-subject SR images with the above equation. The SR images for 6 of the 8 subjects were averaged, excluding the two aforementioned subjects with short interscan intervals.

Ex vivo SV2A quantification with Western blots

Near-term fetal tissues were harvested as described previously [28]. Samples collected for Western blot were frozen over liquid nitrogen and shipped by overnight delivery from Site 2 to Site 1 for ex vivo analyses. Nineteen samples per animal were obtained from the following regions: prefrontal (2), frontal (2), parietal (2), temporal (2), occipital (2) cortices, caudate (1), putamen (1), hippocampus (1), amygdala (1), thalamus (2), cerebellum (2), and white matter (1). Samples were prepared for Western Blotting using the Wes Simple Western system (ProteinSimple, CA, USA) as described in Online Resource 1 to obtain a normalized SV2A measure for each sample. In short, the SV2A peak areas from each Western experiment were normalized to the SV2A peak area of a reference sample, which was designated as an excess brain sample from the occipital cortex of one representative subject and was analyzed in each Western experiment to control for inter-experiment variability. For each region, the normalized SV2A density was averaged across all four fetuses to obtain the average normalized SV2A peak area, and correlation analysis was performed with this measure and the average SV2A PET ROI measurements of DVR obtained at 145 days gestational age. To compare the in utero SV2A concentrations to those in the fully developed adult monkey brain, a total of five previously dissected samples across four GM regions (frontal cortex, occipital cortex, thalamus, and cerebellum) from two adult rhesus were utilized (5- and 13-year-old males). Western blot experiments were completed and quantified as described in Online Resource 1. The adult SV2A measures (average of N = 5 normalized SV2A regional measures) were used to normalize regional SV2A measures in the fetal brain to estimate an ex vivo fetal-to-adult SV2A ratio, analogous to the in vivo fetal-to-adult SV2A PET DVR. To correct for non-displaceable radiotracer binding in the DVR measure, we consider an in vivo specific V_S ratio, $V_S^{Fetal}/V_S^{Maternal}$ based on the DVR, as described in Online Resource 1.

Statistical analysis

To evaluate whether methodological differences across the scan sites (due to scanner and tracer variations) introduced significant differences in the datasets, unpaired *t*-tests were completed with the area under the curve (AUC) of the maternal GM TAC from scan 1 for all subjects in units of standardized uptake value (SUV, g/cm^3) from 10- to 30-min post-radiotracer injection. Paired *t*-tests were used with the same measure within subject to evaluate any statistically significant difference between scan 1 at 120 days and scan 2 at 145-days gestational age, and to evaluate differences between average cortical and subcortical DVRs within scans. The dam brain uptake was used for these analyses as the SV2A density is not expected to change between scans during adulthood. Further, since the maternal brain is used as a reference region in the kinetic modeling analysis, we ensured that the reference region did not introduce any variability. Descriptive statistics are reported as mean (± SD) unless stated otherwise. Statistical analyses were completed in GraphPad Prism (Graph-Pad Software).

Results

No significant differences in maternal brain uptake across imaging sites or tracer administration protocols

To examine whether any scan site differences may contribute to variability in the PET outcome measures, we performed a primary statistical analysis on the maternal GM TACs in units of standardized uptake value (SUV, g/mL) between scans completed at the Yale PET Center (Site 1, $N = 8$ scans; $N = 4$ animals) and UC Davis (Site 2, $N = 8$ scans; $N = 4$ animals). There were no differences in average maternal brain AUC observed between imaging sites (Site 1: 211 (± 126) g/mL × min; Site 2: 157 (± 41) g/mL × min; $t(6) = 0.812$, $p = 0.44$). There was also no significant difference in average maternal brain AUC between bolus plus infusion (B + I, $N = 2$) and bolus (B, $N = 6$) radiotracer administration paradigms (B + 1: 268 (± 181) g/mL × min; B: 156 (± 36) g/mL × min; $p = 0.543$).

No significant differences in maternal brain uptake within subject across scans

Within-subject changes in fetal brain SV2A density might be explained by differences in uptake of the radioligand in the dam. We compared the AUC of the maternal GM TAC across the two scans for each subject, but did not observe any significant differences, with average percent difference between each subjects' two scans of 6.4% (± 24.%, $t(7) = -0.03$, $p = 0.97$). These data, as well as the lack of significant differences in maternal brain uptake across scan sites, suggest that the maternal brain could serve as a control and a within-scan reference to quantify fetal brain SV2A PET uptake.

Total body imaging of the gravid rhesus macaque with SV2A PET

All eight animals successfully underwent SV2A PET imaging twice during the third trimester, resulting in total body images for quantitative analysis of the fetal brain. The injected dose of the PET radioligand was 166 ± 43 MBq (4.5 ± 1.2 mCi) for [^{11}C]UCB-J scans at Site 1 and 3.1 ± 0.3 mCi (113 ± 12 MBq) for [^{18}F]SynVesT-1 scans at Site 2. PET scanning with both [^{11}C]UCB-J and [^{18}F] SynVesT-1 resulted in expected whole-body

uptake, notably in the maternal brain, liver, and kidneys, consistent with previous primate dosimetry scans. Additionally, both SV2A tracers crossed the placenta and entered the fetal circulation as radiotracer uptake was observed within the fetal brain and the fetal liver within 1 min of radiotracer administration. SUV images for a gravid monkey in the third trimester (120 and 145-days gestational age; term 165 ± 10 days) are shown for [^{18}F]SynVesT-1 scans in Fig. 1.

Fetal brain SV2A increases during the third trimester

A sagittal view of the fetal brain is shown in Fig. 1 inserts (120- and 145-days gestational age). Example regional time activity curves and corresponding Logan fits are shown in Online Resource 3A and 3B, respectively. No differences in measures of fetal whole brain DVR were observed across site at either time point with average DVRs of 0.147 (± 0.023) and 0.121 (± 0.055) for Site 1 and Site 2 respectively at the first scan ($p = 0.41$), and 0.217 (± 0.035) and 0.213 (± 0.047) for Site 1 and Site 2, respectively at the second scan ($p = 0.89$). Across the two sites, there was a significant difference in interscan interval, with average age difference between scans of 28 (± 5) at Site 1 and 18 (± 5) at Site 2 ($p = 0.027$). From both sites, DVR measures increased between the early and late third trimester for all fetal brains. On average, the percent increase in DVR between the two scans was 75 ± 69%, with some animals showing over 100% increase from the scan 1 DVR (Fig. 2, paired t-test $t(7) = -5.09$, $p = 0.0014$).

Heterogeneous SV2A PET tracer distribution in the fetal brain

Regional DVR information was obtained from the PET data after aligning to the neonate rhesus macaque magnetic resonance (MR) template [24]. SV2A radiotracer distribution was heterogenous in the fetal brain (Fig. 3). The highest SV2A tracer binding was localized to subcortical and midbrain regions of the brain, with lower uptake in the frontal and occipital cortices and cerebellum. At both time points, the subcortical regional average ($N = 5$ regions including the thalamus, caudate, and putamen) was greater than average cortical DVR ($N = 6$ regions including the prefrontal, frontal, and temporal cortices) with average ($N = 8$) DVRs of 0.256 (± 0.034) and 0.163 (± 0.023), respectively, at 120 days gestational age ($p < 0.001$), and 0.380 (± 0.056) and 0.274 (± 0.060), respectively, at 145 days gestational age ($p < 0.001$). Higher SV2A PET uptake in subcortical regions of the fetal brain was also observed in average parametric images of DVR at both gestational ages (Fig. 3A, B).

SV2A uptake was also quantified in functionally distinct anatomical subdivisions of primary and associative cortices (somatosensory, motor, visual) [25], to investigate differences in SV2A density across functional brain regions. Primary regions tended to have higher DVR than association regions at both time points, although this was not consistent across functional areas. For example, the DVR at 120 days gestational age in the primary somatosensory region was less than the associative, with average ($N = 8$) DVRs of 0.173 (± 0.043) and 0.194 (± 0.048), respectively ($p = 0.050$). In the motor areas, the DVR in the primary region was greater than the DVR in the associative, with average DVRs of 0.195 (± 0.052) and 0.163 (± 0.038), respectively ($p = 0.008$). Lower values of DVR were observed in the visual cortex, where the DVR in the primary region tended to be greater than that of the associative on average, with DVRs of 0.163 (± 0.058) and 0.145 (± 0.027), respectively,

although this trend was not significant ($p = 0.458$). The DVR at 145 days gestational age in primary somatosensory region was greater than the associative, with average DVRs of 0.352 (± 0.056) and 0.333 (± 0.065), respectively, although these trends were not significant ($p = 0.123$). Significant differences were observed between the DVR in primary and associative regions in the motor areas, with average values of 0.356 (± 0.060) and 0.293 (± 0.063) respectively ($p < 0.001$), and in the visual regions with average DVRs of 0.242 (± 0.044) and 0.249 (± 0.043), respectively ($p = 0.010$). Regional DVR estimates in the fetal brain are reported for cortical, subcortical, and functional ROIs in Tables 2 and 3. These results show SV2A density differs across the macaque cerebral cortex throughout the third trimester.

Quantification of synaptogenesis rates in the fetal brain

Synaptogenesis rates are shown in Tables 2 and 3. Parametric images of SR are shown in Fig. 3C. Individual and average ($N = 8$) regional DVR increases are shown for all ROIs in Fig. 4. Most notably, subcortical and midbrain regions also appeared to have higher rSR compared to cortical regions. Additionally, rSR was relatively higher in the sensorimotor regions, while other cortical regions such as prefrontal and occipital cortices showed lower rates of increase. Quantitatively, when excluding two subjects with a shorter interscan interval, the average ($N = 6$) rSR values in subcortical regions were similar to rSR in cortical regions, with rSR of 0.004 (± 0.003) and 0.004 (± 0.002), respectively ($p = 0.520$). In the somatosensory cortex, there was a trend of higher rSR in primary regions than in associative regions, with rSR values of 0.007 (± 0.002) and 0.006 (± 0.002), respectively, though this was not significant ($p = 0.104$). The motor cortex also had an insignificant trend of slightly higher rSR in primary regions compared to associative regions with average rSRs to 0.0055 (± 0.0017) and 0.0051 (± 0.0022), respectively ($p = 0.405$). In the visual cortex, the rSR in primary regions tended to be lower than in the associative regions, with respective average rSR values of 0.0029 (± 0.0026) and 0.0040 (± 0.0016), though this trend was also not statistically significant ($p = 0.352$). These results suggest that SV2A changes occur at largely similar rates across the fetal brain.

Ex vivo SV2A measures correlated with in vivo SV2A measurements

Regional fetal brain samples of four rhesus fetuses were used to explore the relationship between the image-derived SV2A concentrations in the fetal brain quantified by DVR with the SV2A concentration derived from Western blotting. Western blot results from a representative subject are shown in Online Resource 4. On average, these measures were well correlated ($R^2 = 0.363$, $p = 0.038$, Online Resource 5A). Thus, the image-derived measures of SV2A agreed well with the true concentrations of SV2A in the fetal brain.

In vivo fetal-to-adult SV2A PET DVR correlates with ex vivo fetal-to-adult SV2A ratio

In order to compare our ex vivo SV2A results to previously reported measures of fetal-to-adult synaptic density levels, we quantified SV2A protein levels in brain tissue previously collected from other adult monkeys using Western blotting. The average SV2A density across four regions (occipital cortex, frontal cortex, thalamus, and cerebellum) was used to normalize the regional ex vivo SV2A concentrations from the fetal brain. The average ($N = 12$ regions) regional ex vivo fetal-to-adult SV2A ratio derived from Western blotting was 0.30 (± 0.12), ranging from ~ 0.13 in the white matter to 0.55 in the thalamus. This

agreed well with the average in vivo fetal-to-adult SV2A DVR of 0.34 (± 0.07). The in vivo SV2A PET DVR of fetal-to-adult brain correlated well with the ex vivo SV2A ratio of fetal-to-adult brain (R^2 = 0.363, p = 0.038, Fig. 5). When applying the approximation to average regional DVR to eliminate the non-displaceable component of the PET signal, the relationship between the in vivo specific $V_S^{fetal}/V_S^{maternal}$ ratio and the ex vivo SV2A ratio remained significant (R^2 = 0.363, p = 0.038; Online Resource 5B). The average regional in vivo $V_S^{fetal}/V_S^{maternal}$ ratio was 0.19 (± 0.08), somewhat less than Western blot ratio of 0.30, likely attributable to PET partial volume effects.

Discussion

The current study is the first report of SV2A PET imaging in the developing fetal rhesus brain. Across two imaging sites, [^{11}C]UCB-J or [^{18}F]SynVesT-1 PET tracers were used to scan a total of 8 gravid rhesus monkeys (4 per site) twice during the third trimester. SV2A PET measures of fetal-to-maternal brain DVR increased within the whole fetal brain and across all regions, which agrees with previous studies in rhesus that have reported increases in synapse number per unit area across the cortex in the fetal brain during the final weeks of gestation as evaluated by electron microscopy [4–8]. At both 120- and 145-days gestational age, DVR measures were higher in most subcortical regions than in cortical regions. This pattern of greater subcortical synaptic density has previously been reported both in terms of synaptic density in the ~ 14-day-old rodent [29] and also agrees with patterns of glucose metabolism in the newborn human determined using [^{18}F] Fluoro-deoxy-glucose (FDG)-PET [30, 31]. The regional DVR values at 145 days gestational age were significantly correlated with ex vivo regional fetal brain SV2A concentrations from Western blotting, providing evidence that measures derived from SV2A PET directly relate to SV2A protein concentrations in the fetal brain. However, the values of DVR reported here conflict with microscopy studies, such that the synaptic density levels reported previously approach or reach 100% of values for adults at the time of birth [4–8], while the DVR values reach about 40% of the adult value. Given that both the ex vivo and in vivo fetal-to-adult SV2A ratios do not agree with previous synaptic density literature, it is possible that SV2A density is a meaningful, but not a direct, estimate of synaptic density in brain development.

In addition to observing SV2A uptake measures, we also report synaptogenesis rates by region and by voxel. We expect that the large range of interscan interval (21–33 days) contributed to some of the variability in our rSR estimates. The rSR values across general cortical areas were largely similar to each other, a trend that has been reported across primary motor, visual, and somatosensory areas in the rhesus monkey using synaptic density measures [6]. Notably, reports of concurrent cortical synaptogenesis in monkeys are not similar to reports in humans, where synaptic density increases more rapidly in primary areas such as the auditory cortex than in areas with higher-order executive functions such as the prefrontal cortex [2]. The outcome measure of DVR is a ratio of total volume of distribution (a sum of specific radiotracer binding, V_S + nondisplaceable binding, V_{ND}) of the region of interest and the reference region. Assuming the nondisplaceable volume of distribution V_{ND} is the same in the fetal and maternal brains and does not change across scans, the increase in

DVR during gestation, as measured here by rSR, reflects an increase in SV2A density, V_S in the fetal brain.

Previous studies have utilized techniques including electron microscopy [4, 32] and more recently immunohistochemistry [33] to assess synaptic density across the brain on a microscale. The outcome measures from these methods represent the quantity of fully developed synapses, with pre- and post-synaptic components, per unit area. The current study implemented a method to evaluate in vivo SV2A, a presynaptic vesicle protein. The increased expression of SYN, another presynaptic vesicle protein which localizes with SV2A [20], has previously been reported to correlate with synaptogenesis as evaluated by electron microscopy in the developing mouse visual cortex [34]. Thus, it is likely that changes in SV2A expression represent the development of mature synapses. However, the differences between fetal-to-adult SV2A ratio, reported here by in vivo PET measures and ex vivo Western blotting, and fetal-to-adult synaptic density levels may be due to increases in SV2A protein expression during brain development, potentially at a rate independent from fully formed synaptic contacts. Previous studies have reported increased SV2A expression by Western blot early in the mouse [35] and in the rat hippocampus [36]. In addition to changes in SV2A protein expression during development, the number of synaptic vesicles per synapse, quantified with electron microscopy, increases during the first month of life, when rodent brain development is more comparable to prenatal development in primates [37], in the rat parietal cortex [38] and visual cortex [39]. With SV2A localized to presynaptic vesicles, changes in vesicle density are likely to affect SV2A density. Furthermore, in the adult rat, approximately 2–5 SV2 proteins per vesicle have been reported [40, 41], but whether this value changes with brain development is not known. Despite these potential dynamic changes during development, following SV2A trajectories throughout the synaptogenesis period remains valuable, due to the protein's importance in normal brain function [42] and particularly if changes in SV2A are related to changes in mature synapse density.

To validate in vivo PET measurements, SV2A protein concentrations were estimated by Western blot using fetal brain samples from a subset of subjects. The positive, significant correlation between in vivo regional SV2A PET measures and ex vivo regional SV2A concentrations was expected, as previous work by our group has shown agreement between in vivo SV2A PET measures and ex vivo SV2A protein concentration in the adult baboon brain [20]. When the ex vivo fetal SV2A concentrations were normalized to the average ex vivo SV2A concentration in the adult monkey, the ex vivo fetal-to-adult SV2A specific ratio also agreed very well with the in vivo fetal-to-adult SV2A PET DVR. The correlation between these two measures was positive (Fig. 5), but there was evidence of non-specific signal in the PET measures. When correcting the DVR to estimate a specific V_S ratio, this relationship remained significant, and the intercept of the regression line approached zero (Online Resource 5B). The in vivo V_S ratio was lower than the observed ex vivo fetal-to-adult SV2A ratio, with a regional average of 0.19 (± 0.08) compared to 0.30 (± 0.12), respectively. This difference may be attributed to partial volume effects (PVE) in the PET images, which results from limited spatial resolution of PET. PVE leads to inaccurate quantitative measures, particularly when imaging small regions or tissues [43], such as small fetal brain regions like the amygdala, which had high variability in DVR across some

scans (Fig. 4). Based on the radiotracer uptake patterns in the fetal brain, it is most likely that spill-over of radioactivity from subcortical and midbrain regions will contribute to quantitative inaccuracies, leading to an underestimation of DVR and thus, a lower calculated in vivo V_S ratio.

It is important to note some variables and limitations related to these studies. First, PET images were acquired at two imaging sites where different sedation protocols were used and PET images were acquired using different PET tracers and scanners. However, given these differences, we did not detect any statistically significant differences in PET measures in the maternal brain; thus, the likelihood of the sites introducing variability in this study is low. One key reason for this difference in radiotracer across sites was that [^{18}F]SynVesT-1 was not yet validated when data collection began at Site 1. However, given the similarity between the two tracers in chemical structure, kinetic profiles, and distribution patterns in the rhesus [15], this difference should not introduce significant bias. Second, there may be differences in the delivery rate of radiotracer between the maternal and fetal brains due to the placenta and the maternal and fetal circulations. The PET data were quantified using a Logan Graphical Method with a t^* of 10 min to account for any potential delay in radiotracer delivery to the fetal brain, relative to the maternal brain. Third, the maternal GM was used as a reference region to attain a fetal-to-adult SV2A outcome measure of DVR. Although the white matter region of the centrum semio-vale (CS) may be a useful reference region for SV2A PET quantification [44], neither the white matter of the maternal brain nor the fetal brain was used as a reference region, due to considerable PVE in each of the regions, which would lead to overestimations of radiotracer concentrations in the reference region due to the small CS region and the poor spatial resolution of the PET system. Future studies may consider exploring these regions as a reference region after correction for PVE. Further validation would also be needed to use the CS of the fetal brain as a reference region in brain development, as myelination of axons across the white matter also occurs during this developmental time period [45]. Increased myelin may introduce variations in tissue properties and characteristics (e.g., lipophilicity) that may affect nonspecific binding of [^{11}C]UCB-J, which has been suggested to be greater in the white matter than in the GM, potentially due to differences in tissue properties [44]. Fourth is the reliance on CT versus structural MRI. To minimize study impact and burden on the dam and the fetus, MRI scans were not performed. Although CT images provide the anatomical delineation of the fetal skull in this study, the images lack soft-tissue contrast that could assist with image processing steps, including nonlinear registration of the fetal brain to the regional template. This may lead to slight inaccuracies in volume of interest definition; however, each registration was reviewed for quality before incorporating into the results of the current study. The lack of MRI also prevented the implementation of partial volume correction techniques, which would have helped improve the reliability of the regional outcome measures, as well as aid in controlling for the increasing fetal brain size during the third trimester. Fifth is our estimate of SV2A change during the late gestation period as a synaptogenesis rate (SR). Since only two measurements per subject during this critical period of brain development for the current study, the overall change in SV2A was defined as the change in SV2A PET DVR within each region/subject, normalized by the difference in gestational age between scans, or the interscan interval. The interscan interval differed

somewhat across subjects due to scheduling, and we believe that it is important to account for this variation when discussing the change in SV2A measures. Thus, we interpret the SR measure as a rate of change between two timepoints. Future studies may consider acquiring additional scans during the second and third trimesters in order to measure the potential nonlinear changes in synaptic density by SV2A in the developing fetal brain. Sixth is the use and validation of SV2A, a presynaptic vesicle protein, as a synaptic marker as previously discussed. The in vivo to ex vivo comparison of SV2A measures completed here was conducted at a single timepoint during gestation (approximately 145 days gestational age). Further studies should explore this comparison at additional periods of brain development. Furthermore, ongoing and future work in our group will focus on validating SV2A as a synaptic marker along with SYN and post-synaptic markers such as post-synaptic density marker PSD-95 and gephyrin. Lastly, the ex vivo validation step in which the fetal brain SV2A concentrations from Western blots used adult brain tissue from two male monkeys for normalization and estimation of the ex vivo fetal-to-adult SV2A ratio, which may introduce variability between the in vivo and ex vivo ratios, due to potential sex differences in the SV2A measures. However, prior work has not reported significant effects of sex on SV2A measures in human [18, 46, 47].

The current study validates a method measuring SV2A in the developing rhesus monkey brain using PET. PET imaging has been previously used in the gravid monkey to image glucose metabolism in the fetal monkey under baseline conditions [48] and under exposure to cocaine [49] using [^{18}F]FDG PET, which reflects fetal neuronal activity to explore potential effects of drug exposure in utero in the fetal brain. A recent study, however, has shown that SV2A-PET is more of a direct measure of synaptic density and may not be as sensitive to changes in neuronal activity [50]. The proposed methodology provides a new technique for performing longitudinal measurements of SV2A density within the same subject at crucial time-points in neurodevelopment. SV2A PET images can be acquired during gestation and after birth, allowing for the potential for both prenatal and postnatal SV2A quantification in the developing brain. Figure 6 shows a fetal SV2A image acquired in the late third trimester alongside an SV2A image in the same subject at two weeks after birth on the Focus220 microPET system, each in units of respective standardized uptake value (SUV). With this, we can continuously monitor SV2A changes in the healthy brain across critical developmental periods, both prenatally and postnatally. Ongoing work will continue to explore and validate SV2A density changes throughout the postnatal period. Furthermore, these methods could be used to explore SV2A in relation to neurodevelopmental disorders that may be associated with preterm birth [4], infectious diseases [28], prenatal stressors [51], or environmental factors such as fetal alcohol or recreational drug exposure [29, 51]. This work shows the capability of PET imaging with SV2A-specific radioligands to evaluate SV2A density in the fetal brain. This method is less invasive than current standards for evaluation of synaptic density during development and allows for longitudinal, within-subject assessment of critical processes in brain development in health or disease.

Supplementary Material

Refer to Web version on PubMed Central for supplementary material.

Acknowledgements

The authors acknowledge the nonhuman primate team at the Yale PET Center, including Daniel Holden, Cynthia Santaniello, Courtney Chabina, Kristin Koehl-Carabetta, and Amanda Harsche, for their assistance in completing the PET studies. The authors also acknowledge Dr. Alvaro Duque and the Rakic Breeding Colony for their assistance with NHP breeding at Yale and the staff at the California National Primate Research Center.

Funding

These studies were supported by National Institutes of Health (NIH) grants (no. MH120615 [SG], and no. U42-OD027094 [AT]), and the California National Primate Research Center base operating grant (no. OD011107). In vivo imaging was performed with instrumentation funded by the NIH (S10 grants RR029245, OD016261, and RR025063), and supported through the Primate Center Multimodal Imaging Core.

Availability of data and material

The raw data and datasets used and/or analyzed in the current study will be made available upon reasonable request to the corresponding and participating authors as deemed appropriate, and in line with the data sharing policy.

References

1. Huttenlocher PR. Synaptic density in human frontal cortex — developmental changes and effects of aging. Brain Res. 1979;163:195–205. 10.1016/0006-8993(79)90349-4. [PubMed: 427544]
2. Huttenlocher PR, Dabholkar AS. Regional differences in synaptogenesis in human cerebral cortex. J Comp Neurol. 1997;387:167–78. 10.1002/(sici)1096-9861(19971020)387:2<167::aid-cne1>3.0.co;2-z. [PubMed: 9336221]
3. Huttenlocher PR, de Courten C, Garey LJ, Van der Loos H. Synaptogenesis in human visual cortex–evidence for synapse elimination during normal development. Neurosci Lett. 1982;33:247–52. 10.1016/0304-3940(82)90379-2. [PubMed: 7162689]
4. Bourgeois JP, Jastreboff PJ, Rakic P. Synaptogenesis in visual cortex of normal and preterm monkeys: evidence for intrinsic regulation of synaptic overproduction. Proc Natl Acad Sci U S A. 1989;86:4297–301. 10.1073/pnas.86.11.4297. [PubMed: 2726773]
5. Bourgeois JP, Rakic P. Changes of synaptic density in the primary visual cortex of the macaque monkey from fetal to adult stage. J Neurosci. 1993;13:2801–20. [PubMed: 8331373]
6. Rakic P, Bourgeois JP, Eckenhoff MF, Zecevic N, Goldman-Rakic PS. Concurrent overproduction of synapses in diverse regions of the primate cerebral cortex. Science. 1986;232:232–5. 10.1126/science.3952506. [PubMed: 3952506]
7. Zecevic N, Bourgeois JP, Rakic P. Changes in synaptic density in motor cortex of rhesus monkey during fetal and postnatal life. Brain Res Dev Brain Res. 1989;50:11–32. 10.1016/0165-3806(89)90124-7. [PubMed: 2582602]
8. Zecevic N, Rakic P. Synaptogenesis in monkey somatosensory cortex. Cereb Cortex. 1991;1:510–23. 10.1093/cercor/1.6.510. [PubMed: 1822755]
9. Murray RM, O'Callaghan E, Castle DJ, Lewis SW. A neurodevelopmental approach to the classification of schizophrenia. Schizophr Bull. 1992;18:319–32. 10.1093/schbul/18.2.319. [PubMed: 1377834]
10. Volk DW, Edelson JR, Lewis DA. Altered expression of developmental regulators of parvalbumin and somatostatin neurons in the prefrontal cortex in schizophrenia. Schizophr Res. 2016;177:3–9. 10.1016/j.schres.2016.03.001. [PubMed: 26972474]
11. Volk DW, Lewis DA. Early developmental disturbances of cortical inhibitory neurons: contribution to cognitive deficits in schizophrenia. Schizophr Bull. 2014;40:952–7. 10.1093/schbul/sbu111. [PubMed: 25053651]
12. Weinberger DR. Implications of normal brain development for the pathogenesis of schizophrenia. Arch Gen Psychiatry. 1987;44:660–9. 10.1001/archpsyc.1987.01800190080012. [PubMed: 3606332]

13. Bajjalieh SM, Peterson K, Shinghal R, Scheller RH. SV2, a brain synaptic vesicle protein homologous to bacterial transporters. Science. 1992;257:1271–3. 10.1126/science.1519064. [PubMed: 1519064]
14. Nabulsi NB, Mercier J, Holden D, Carre S, Najafzadeh S, Vandergeten MC, et al. Synthesis and preclinical evaluation of 11C-UCB-J as a PET tracer for imaging the synaptic vesicle glycoprotein 2A in the brain. J Nucl Med. 2016;57:777–84. 10.2967/jnumed.115.168179. [PubMed: 26848175]
15. Li S, Cai Z, Wu X, Holden D, Pracitto R, Kapinos M, et al. Synthesis and in vivo evaluation of a novel PET radiotracer for imaging of synaptic vesicle glycoprotein 2A (SV2A) in nonhuman primates. ACS Chem Neurosci. 2019;10:1544–54. 10.1021/acschemneuro.8b00526. [PubMed: 30396272]
16. Chen MK, Mecca AP, Naganawa M, Finnema SJ, Toyonaga T, Lin SF, et al. Assessing synaptic density in Alzheimer disease with synaptic vesicle glycoprotein 2A positron emission tomographic imaging. JAMA Neurol. 2018;75:1215–24. 10.1001/jamaneurol.2018.1836. [PubMed: 30014145]
17. Mecca AP, Chen MK, O'Dell RS, Naganawa M, Toyonaga T, Godek TA, et al. In vivo measurement of widespread synaptic loss in Alzheimer's disease with SV2A PET. Alzheimers Dement. 2020;16:974–82. 10.1002/alz.12097. [PubMed: 32400950]
18. Holmes SE, Scheinost D, Finnema SJ, Naganawa M, Davis MT, DellaGioia N, et al. Lower synaptic density is associated with depression severity and network alterations. Nat Commun. 2019;10:1529. 10.1038/s41467-019-09562-7. [PubMed: 30948709]
19. Finnema SJ, Toyonaga T, Detyniecki K, Chen MK, Dias M, Wang Q, et al. Reduced synaptic vesicle protein 2A binding in temporal lobe epilepsy: A [(11) C]UCB-J positron emission tomography study. Epilepsia. 2020;61:2183–93. 10.1111/epi.16653. [PubMed: 32944949]
20. Finnema SJ, Nabulsi NB, Eid T, Detyniecki K, Lin SF, Chen MK, et al. Imaging synaptic density in the living human brain. Sci Transl Med. 2016;8:348ra96. 10.1126/scitranslmed.aaf6667.
21. Tarantal AF (2005) Ultrasound Imaging in Rhesus (*Macaca mulatta*) and Long-Tailed (*Macaca fascicularis*) Macaques. Reproductive and Research Applications. In: The Laboratory Primate, Ch. 20. Elsevier Academic Press, Cambridge, pp 317–315
22. Berg E, Gill H, Marik J, Ogasawara A, Williams S, van Dongen G, et al. Total-body PET and highly stable chelators together enable meaningful (89)Zr-antibody PET studies up to 30 days after injection. J Nucl Med. 2020;61:453–60. 10.2967/jnumed.119.230961. [PubMed: 31562219]
23. Berg E, Zhang X, Bec J, Judenhofer MS, Patel B, Peng Q, et al. Development and evaluation of mini-EXPLORER: a long axial field-of-view PET scanner for nonhuman primate imaging. J Nucl Med. 2018;59:993–8. 10.2967/jnumed.117.200519. [PubMed: 29419483]
24. Young JT, Shi Y, Niethammer M, Grauer M, Coe CL, Lubach GR, et al. The UNC-Wisconsin Rhesus Macaque Neurodevelopment Database: a structural MRI and DTI database of early postnatal development. Front Neurosci. 2017;11:29. 10.3389/fnins.2017.00029. [PubMed: 28210206]
25. Reveley C, Gruslys A, Ye FQ, Glen D, Samaha J, Russ BE, et al. Three-dimensional digital template atlas of the Macaque Brain. Cereb Cortex. 2017;27:4463–77. 10.1093/cercor/bhw248. [PubMed: 27566980]
26. Logan J, Fowler JS, Volkow ND, Wang GJ, Ding YS, Alexoff DL. Distribution volume ratios without blood sampling from graphical analysis of PET data. J Cereb Blood Flow Metab. 1996;16:834–40. 10.1097/00004647-199609000-00008. [PubMed: 8784228]
27. Bartlett RM, Dejesus OT, Barnhart TE, Nickles RJ, Christian BT, Graner JL, et al. Fetal dopamine receptor characteristics assessed in utero. J Cereb Blood Flow Metab. 2010;30:1437–40. 10.1038/jcbfm.2010.77. [PubMed: 20531464]
28. Tarantal AF, Hartigan-O'Connor DJ, Penna E, Kreutz A, Martinez ML, Noctor SC. Fetal Rhesus Monkey first trimester Zika virus infection impacts cortical development in the second and third trimesters. Cereb Cortex. 2021;31:2309–21. 10.1093/cercor/bhaa336. [PubMed: 33341889]
29. Lancaster F, Delaney C, Samorajski T. Synaptic density of cau-date-putamen and visual cortex following exposure to ethanol in utero. Int J Dev Neurosci. 1989;7:581–9. 10.1016/0736-5748(89)90017-8. [PubMed: 2603756]

30. Chugani HT, Phelps ME. Maturational changes in cerebral function in infants determined by 18FDG positron emission tomography. Science. 1986;231:840–3. 10.1126/science.3945811. [PubMed: 3945811]
31. Chugani HT, Phelps ME, Mazziotta JC. Positron emission tomography study of human brain functional development. Ann Neurol. 1987;22:487–97. 10.1002/ana.410220408. [PubMed: 3501693]
32. Rakic P. Mode of cell migration to the superficial layers of fetal monkey neocortex. J Comp Neurol. 1972;145:61–83. 10.1002/cne.901450105. [PubMed: 4624784]
33. McLeod F, Marzo A, Podpolny M, Galli S, Salinas P. Evaluation of synapse density in hippocampal rodent brain slices. J Vis Exp. 2017. 10.3791/56153.
34. Li M, Cui Z, Niu Y, Liu B, Fan W, Yu D, et al. Synaptogenesis in the developing mouse visual cortex. Brain Res Bull. 2010;81:107–13. 10.1016/j.brainresbull.2009.08.028. [PubMed: 19751806]
35. Crevecoeur J, Foerch P, Doupagne M, Thielen C, Vandenplas C, Moonen G, et al. Expression of SV2 isoforms during rodent brain development. BMC Neurosci. 2013;14:87. 10.1186/1471-2202-14-87. [PubMed: 23937191]
36. Vanoye-Carlo A, Gomez-Lira G. Differential expression of SV2A in hippocampal glutamatergic and GABAergic terminals during postnatal development. Brain Res. 2019;1715:73–83. 10.1016/j.brainres.2019.03.021. [PubMed: 30905653]
37. Clancy B, Darlington RB, Finlay BL. Translating developmental time across mammalian species. Neuroscience. 2001;105:7–17. 10.1016/s0306-4522(01)00171-3. [PubMed: 11483296]
38. Nakamura H, Kobayashi S, Ohashi Y, Ando S. Age-changes of brain synapses and synaptic plasticity in response to an enriched environment. J Neurosci Res. 1999;56:307–15. 10.1002/(SICI)1097-4547(19990501)56:3<307::AID-JNR10>3.0.CO;2-3. [PubMed: 10336260]
39. Blue ME, Parnavelas JG. The formation and maturation of synapses in the visual cortex of the rat II Quantitative analysis. J Neurocytol. 1983;12:697–712. 10.1007/BF01181531. [PubMed: 6619907]
40. Mutch SA, Kensel-Hammes P, Gadd JC, Fujimoto BS, Allen RW, Schiro PG, et al. Protein quantification at the single vesicle level reveals that a subset of synaptic vesicle proteins are trafficked with high precision. J Neurosci. 2011;31:1461–70. 10.1523/JNEUROSCI.3805-10.2011. [PubMed: 21273430]
41. Takamori S, Holt M, Stenius K, Lemke EA, Gronborg M, Riedel D, et al. Molecular anatomy of a trafficking organelle. Cell. 2006;127:831–46. 10.1016/j.cell.2006.10.030. [PubMed: 17110340]
42. Crowder KM, Gunther JM, Jones TA, Hale BD, Zhang HZ, Peterson MR, et al. Abnormal neurotransmission in mice lacking synaptic vesicle protein 2A (SV2A). Proc Natl Acad Sci U S A. 1999;96:15268–73. 10.1073/pnas.96.26.15268. [PubMed: 10611374]
43. Hoffman EJ, Huang SC, Phelps ME. Quantitation in positron emission computed tomography: 1. Effect of object size. J Comput Assist Tomogr. 1979;3:299–308. 10.1097/00004728-197906000-00001. [PubMed: 438372]
44. Rossano S, Toyonaga T, Finnema SJ, Naganawa M, Lu Y, Nabulsi N, et al. Assessment of a white matter reference region for (11)C-UCB-J PET quantification. J Cereb Blood Flow Metab. 2020;40:1890–901. 10.1177/0271678X19879230. [PubMed: 31570041]
45. Tau GZ, Peterson BS. Normal development of brain circuits. Neuropsychopharmacology. 2010;35:147–68. 10.1038/npp.2009.115. [PubMed: 19794405]
46. Carson RE, Naganawa M, Matuskey D, Mecca A, Pittman B, Toyonaga T, et al. Age and sex effects on synaptic density in healthy humans as assessed with SV2A PET. Journal of Nuclear Medicine. 2018;59:541–541.
47. Michiels L, Delva A, van Aalst J, Ceccarini J, Vandenberghe W, Vandenbulcke M, et al. Synaptic density in healthy human aging is not influenced by age or sex: a (11)C-UCB-J PET study. Neuro-image. 2021;232: 117877. 10.1016/j.neuroimage.2021.117877.
48. Benveniste H, Fowler JS, Rooney WD, Moller DH, Backus WW, Warner DA, et al. Maternal-fetal in vivo imaging: a combined PET and MRI study. J Nucl Med. 2003;44:1522–30. [PubMed: 12960202]

49. Benveniste H, Fowler JS, Rooney WD, Scharf BA, Backus WW, Izrailtyan I, et al. Cocaine is pharmacologically active in the nonhuman primate fetal brain. Proc Natl Acad Sci U S A. 2010;107:1582–7. 10.1073/pnas.0909585107. [PubMed: 20080687]

50. Smart K, Liu H, Matuskey D, Chen MK, Torres K, Nabulsi N, et al. Binding of the synaptic vesicle radiotracer [(11)C]UCB-J is unchanged during functional brain activation using a visual stimulation task. J Cereb Blood Flow Metab. 2021;41:1067–79. 10.1177/0271678X20946198. [PubMed: 32757741]

51. Schneider ML, Moore CF, Kraemer GW, Roberts AD, DeJesus OT. The impact of prenatal stress, fetal alcohol exposure, or both on development: perspectives from a primate model. Psychoneuroendocrinology. 2002;27:285–98. 10.1016/s0306-4530(01)00050-6. [PubMed: 11750784]

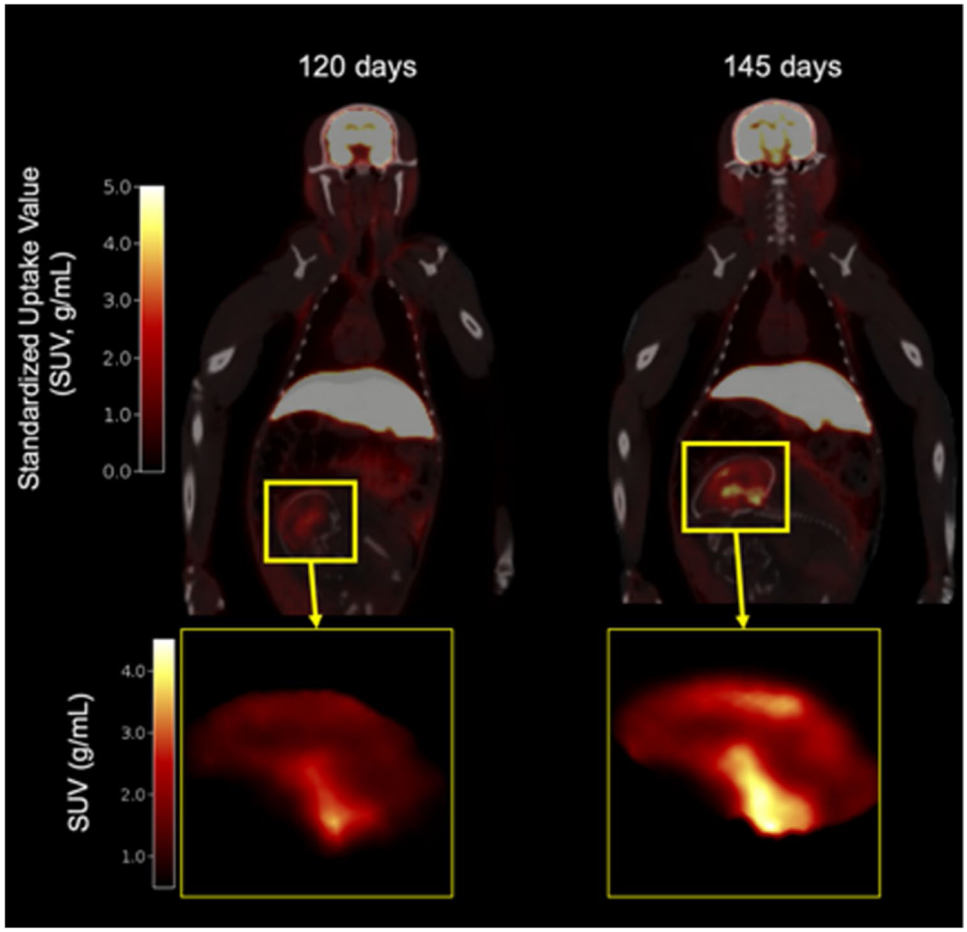

Fig. 1.

Whole-body PET standardized uptake value (SUV) images (10–30 min) of gravid rhesus macaque overlaid on CT at 120 (left) and 145-days gestational age (right). Insert: Sagittal view of fetal brain. Color bar units: SUV (g/mL)

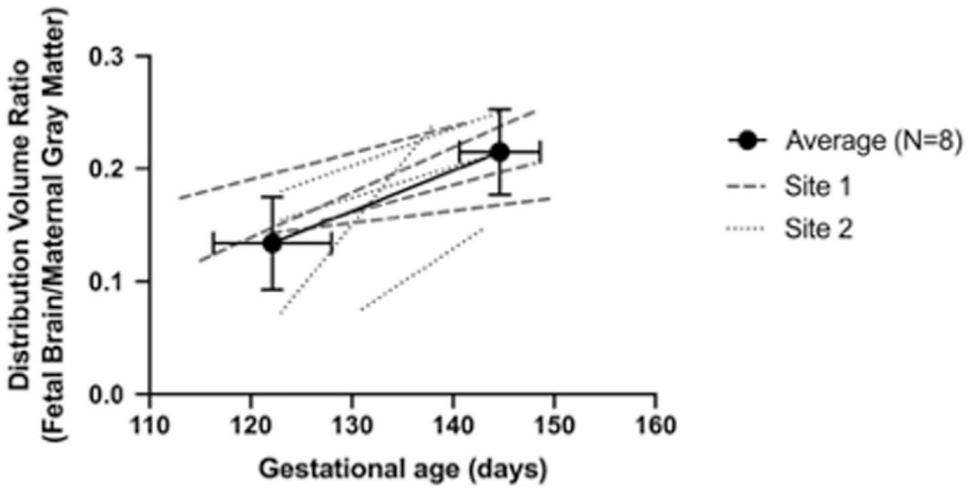

Fig. 2.

Fetal whole-brain DVR increases during the third trimester. Average DVR across the two scans shown with a solid line (error bars are standard deviation across $N = 8$). Individual data points from Site 1 are shown with dashed lines, and individual data points from Site 2 shown with dotted lines. Trimesters are divided by 55-day increments (first trimester 0–55 days, second trimester 56–110 days, and third trimester 111–165 days; term 165 ± 10 days in this species)

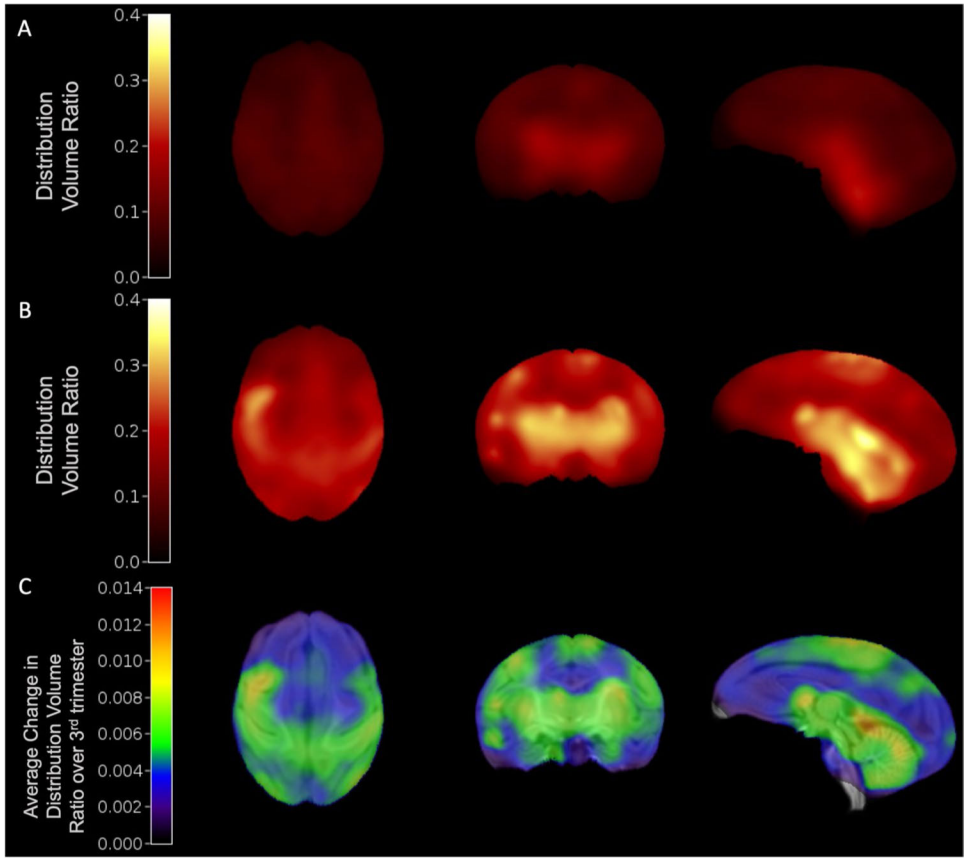

Fig. 3.

Synaptogenesis rates were quantified using average DVR images of the fetal brain. Average (*N* = 6) DVR images at 120-days (**A**) and 145-days gestational age (**B**). **C** Synaptogenesis rate (SR) image across 6 animals, showing the average change in DVR normalized by the change in gestational age between scans during the third trimester (~ 120- to 145-days gestational age), overlaid on neonate MRI template(21)

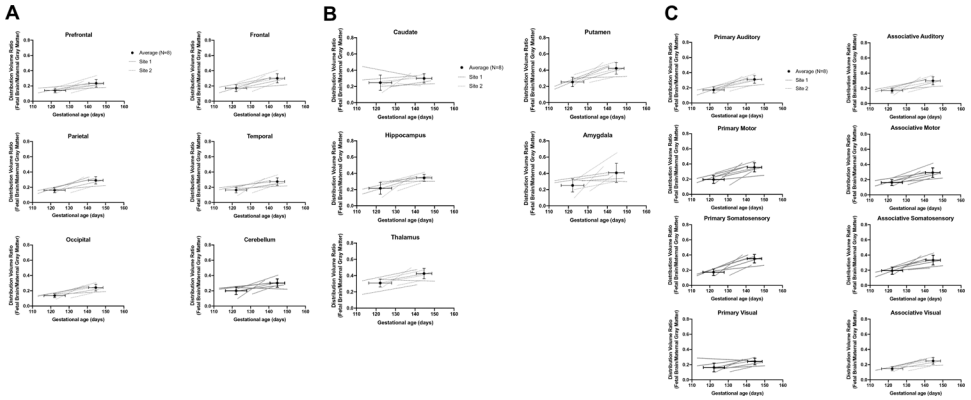

Fig. 4.

Regional fetal brain DVR increases across cortical (**A**), subcortical (**B**), and functional (**C**) ROIs. Average DVRs are shown with a solid line. Individual data points from Site 1 are shown with dashed lines, and individual data points from Site 2 are shown with dotted lines. Error bars are standard deviation across $N = 8$

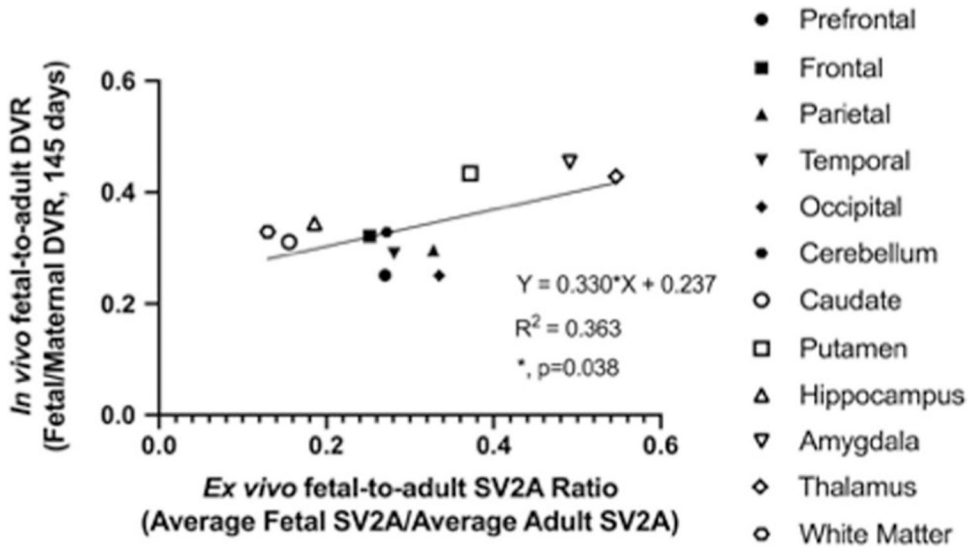

Fig. 5.

Average regional [^{18}F]SynVesT-1 SV2A PET DVR (N = 4) is significantly correlated with average (N = 4) ex vivo fetal-to-adult SV2A ratio

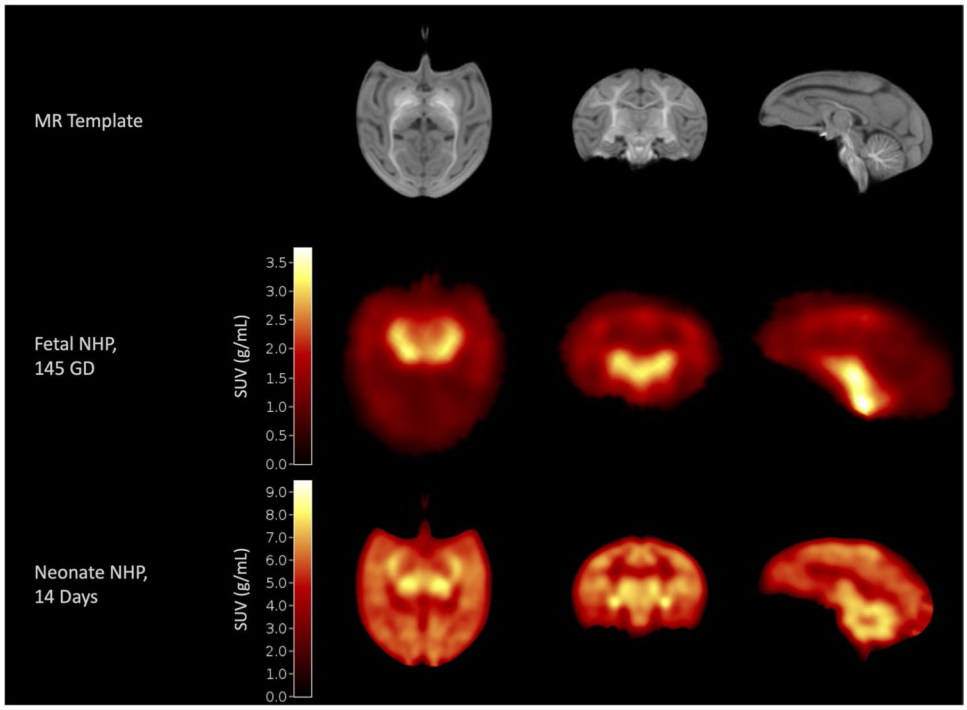

Fig. 6.

SV2A PET uptake patterns are similar between late-gestation and early neonatal period. Neonate Rhesus Macaque Template (top row [24]) with a fetal NHP SV2A image acquired at 145-day gestational age (middle row) and a neonatal SV2A image acquired at 2-week postnatal age (bottom row) in the same subject

Table 1

Table of methodological details of scan sites.

	Site 1	**Site 2**
Scanning location	Yale PET Center, New Haven, CT	UC Davis California National Primate Research Center, Davis, CA
PET imaging system	Siemens Biograph mCT	Primate total-body mini-EXPLORER
Radiotracer (targeted injected dose)	[^{11}C]UCB-J (185 MBq)	[^{18}F]SynVesT-1 (111 MBq)
Sedation/anesthesia protocol	Ketamine/glycopyrrolate + Isoflurane gas	Telazol + Ketamine
Image reconstruction	OSEM (3i21s) with TOF + PSF	OSEM (2i20s) with TOF + PSF

Abbreviations: MBq = mega-Bequerel, OSEM = ordered subset expectation maximization, TOF = time of flight modeling, PSF = point spread function modeling, 2i21s = 2 iterations, 21 subsets, 3i21s = 3 iterations, 21 subsets

Table 2

Average (s.d., $N = 8$) regional DVR estimates for cortical and subcortical fetal brain regions at 120- and 145-days gestational age. Average synaptogenesis rate for each region is shown in the right column

Region	Average (s.d.) DVR, 120 days, $N = 8$	Average (s.d.) DVR, 145 days, $N = 8$	Average (s.d.) rSR (DVR Increase per day)
Prefrontal	0.141 (0.030)	0.234 (0.050)	0.0047 (0.0032)
Frontal	0.172 (0.044)	0.301 (0.059)	0.0064 (0.0036)
Parietal	0.162 (0.033)	0.292 (0.047)	0.0062 (0.0032)
Occipital	0.136 (0.027)	0.242 (0.044)	0.0052 (0.0031)
Temporal	0.164 (0.037)	0.274 (0.049)	0.0057 (0.0045)
Cerebellum	0.200 (0.048)	0.301 (0.055)	0.0056 (0.0053)
Hippocampus	0.216 (0.073)	0.344 (0.043)	0.0065 (0.0051)
Amygdala	0.252 (0.081)	0.406 (0.118)	0.0087 (0.0094)
Caudate	0.247 (0.094)	0.300 (0.057)	0.0030 (0.0063)
Putamen	0.255 (0.058)	0.423 (0.072)	0.0079 (0.0051)
Thalamus	0.309 (0.049)	0.426 (0.063)	0.0058 (0.0048)

Table 3

Average (s.d, $N = 8$) regional DVR estimates for primary and associative cortices at 120- and 145-days gestational age. Average synaptogenesis rate for each region is shown in the right column

Region	Average (s.d.) DVR, 120 days, $N = 8$	Average (s.d.) DVR, 145 days, $N = 8$	Average (s.d.) rSR (DVR Increase per day)
Primary auditory	0.172 (0.040)	0.311 (0.051)	0.0067 (0.0037)
Associative auditory	0.170 (0.031)	0.300 (0.054)	0.0065 (0.0043)
Primary motor	0.195 (0.052)	0.356 (0.060)	0.0082 (0.0053)
Associative motor	0.163 (0.038)	0.293 (0.063)	0.0063 (0.0034)
Primary somatosensory	0.173 (0.043)	0.352 (0.056)	0.0087 (0.0046)
Associative somatosensory	0.194 (0.048)	0.333 (0.065)	0.0064 (0.0046)
Primary visual	0.163 (0.023)	0.242 (0.044)	0.0042 (0.0037)
Associative visual	0.145 (0.027)	0.249 (0.043)	0.0050 (0.0028)